CHAPTER 4

Study on Undulator Radiation

In the future setup of the accelerator system at the PBP-CMU Linac Laboratory, an electromagnetic undulator will be installed downstream the linac structure as a new experimental station. A schematic layout of the future facilty is shown in Fig. 4.1. Study on generation of coherent undulator radiation was perform and the results are presented and discussed in this chapter. Design and construction of the undulator magnet prototype were conducted by K. Thaijai-un [38]. Some important information about the undulator magnet is summarized here as the input data for the calculation of the undulator radiation. Comparison of the radiated power for coherent undulator radiation and trarmsition radiation was done in order to investigate the possibility to increase the power of the THz radiation.

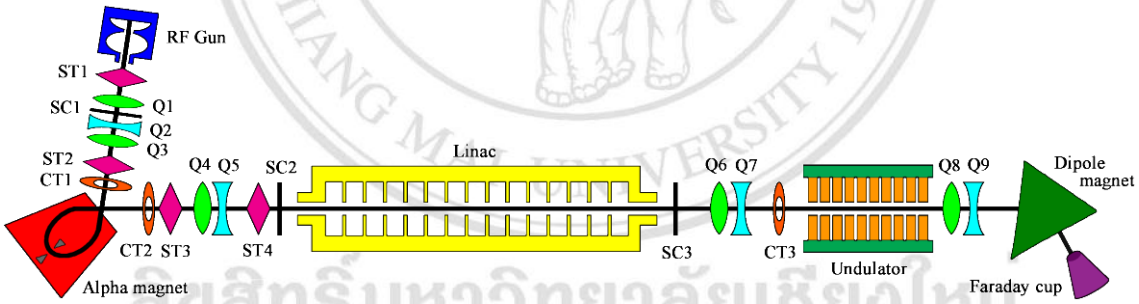

Figure 4.1: Schematic layout of the future accelerator system at the PBP-CMU Linac Laboratory. Dimensions of all components are not scaled.

4.1 Undulator Magnet

4.1.1 Choice of Undulator Period Length and Undultor Parameter

The PBP-CMU Linac system can produce femtosecond electron bunches with a typical electron beam energy of about 8 to 12 MeV. Higher beam energies (15 - 20 MeV) can be achieved with higher feeding RF power. To study the dependence of the undulator parameter on the electron beam energy and the undulator period length, we

considered

electron beams with 4 energy values, which are 10, 12, 15, and 20 MeV. Then, an undulator period length and an undulator parameter were determined by using Equation (2.59) for generation of the THz radiation at the fundamental harmonic $(n=1)$ with selected central wavelength of about 100 μm. The calculated undulator period length as a function of the undulator parameter for different electron beam energies is shown in Fig. 4.2.

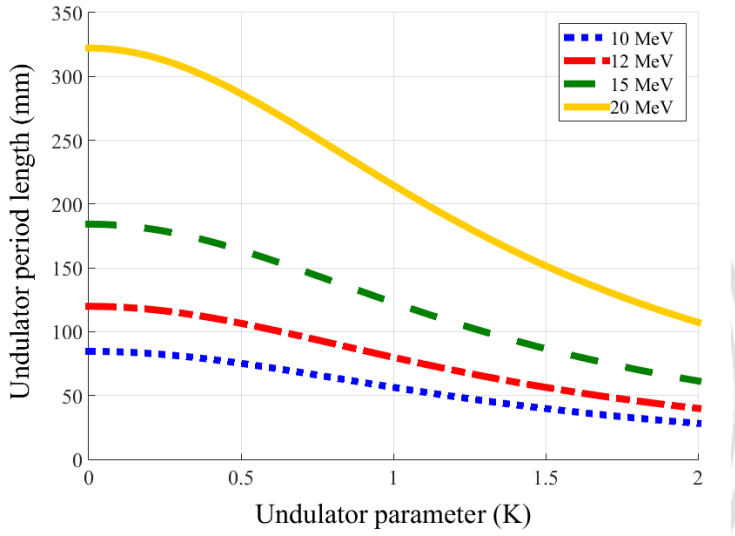

Figure 4.2: Undulator period length as a function of undulator parameter for electron energies of 10, 12, 15 and 20 MeV.

The undulator period length gets longer as the electron energy increases for each undulator parameter. The maximum period length is limited by the length of available space for installation of the undulator magnet, which will be located downstream the linac structure as shown in Fig. 4.1. This available space is around 2 m. In addition, the minimum undulator period length is constrained by the size of the conducting coils that can be energized with an electric current without heating up the coils to have a temperature beyond the insulator limit. From the mentioned conditions, the undulator period length was chosen to be 64 mm, which leads to the total length of about 1.92 m for the undulator magnet with 30 periods. As shown in Fig. 4.2, when we consider the electron beam energy of 10 MeV and the undulator period length of 64 mm, the proper undulator parameter is around 1 (K~1). In order to achieve a magnetic field strength, which provides the desired undulator parameter value, the gap of the undulator magnet was set to be 10.5 mm.

4.1.2 Prototype of Electromagnetic Undulator Magnet

A prototype of planar electromagnetic undulator was designed and constructed by K. Thaijai-un [38]. Both 2D computer code POISSON [39] and 3D computer code RADIA [40] were used to design the undulator magnet. The undulator prototype with the period length of 64 mm has 6 periods composing of 11 main poles and 2 end poles for magnetic field correction at the two ends of the magnet. The pole number was correctly defined to be an odd number in order to have enough number of poles to guide the electron trajectory back to the mid-plane of the magnet. A current density of the conducting coils for the main poles was optimized in order to produce the magnetic field strength with the desired undulator parameter of about unity (K~1). Figure 4.3 shows the three-dimensional RADIA model and the picture of the actual undulator prototype.

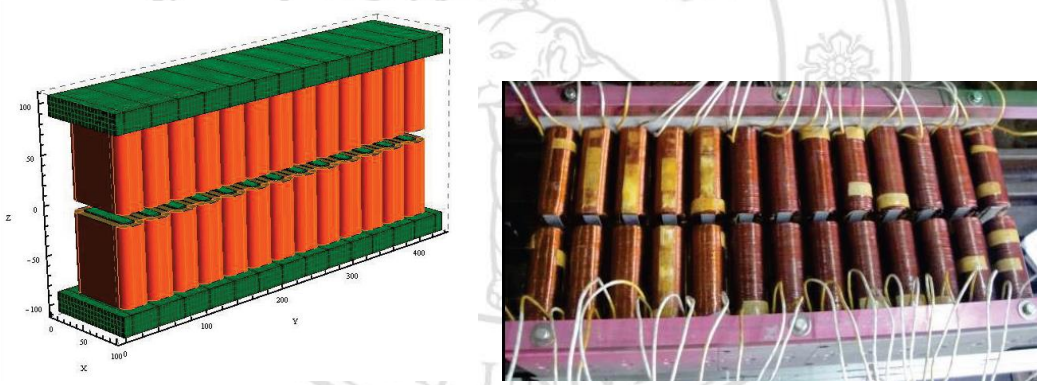

Figure 4.3: 3D RADIA model of undulator prototype with 6 periods (left) and the actual undulator prototype (right) [41].

The prototype of the undulator magnet was constructed according to the design dimensions from simulation results [41]. The magnet poles and yokes were precisely machined with the Computer Numerical Control (CNC) machine. A conducting wire with 515 turns were wired around each undulator pole. The undulator magnetic field was measured by using a Hall's effect teslameter [42]. All magnetic field measurements were performed at the thermal equilibrium state. The magnetic field distribution along the undulator axis for ideal periodic field and the measured result at the excitation current of 1 A are shown together in Fig. 4.4.

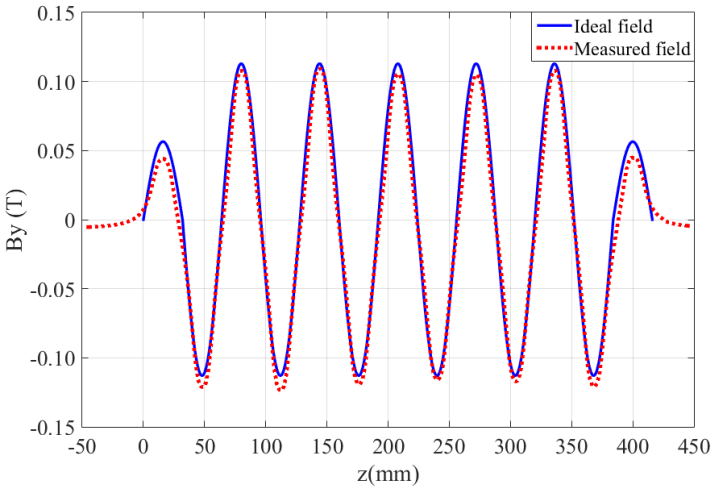

Figure 4.4: Ideal and measured magnetic field distributions on the mid plane along the undulator axis at an excitation current of 1 A [41].

The peak magnetic field of the undulator prototype can be varied by adjusting the applied current of the conducting coils, which is limited by the specification of the power supply. The measurement result shows that the peak magnetic field of 50 - 167 mT corresponding to the undulator parameter of 0.3 - 1.0 can be obtained. Thus, the undulator radiation of 87 - 125 μm can be achieved for 10 MeV electron beam [41]. Moreover, the first and the second integration of the ideal and the measured undulator magnetic fields were done to obtain an angular displacement (Fig. 4.5) and a horizontal displacement (Fig. 4.6) of the electron along the undulator axis.

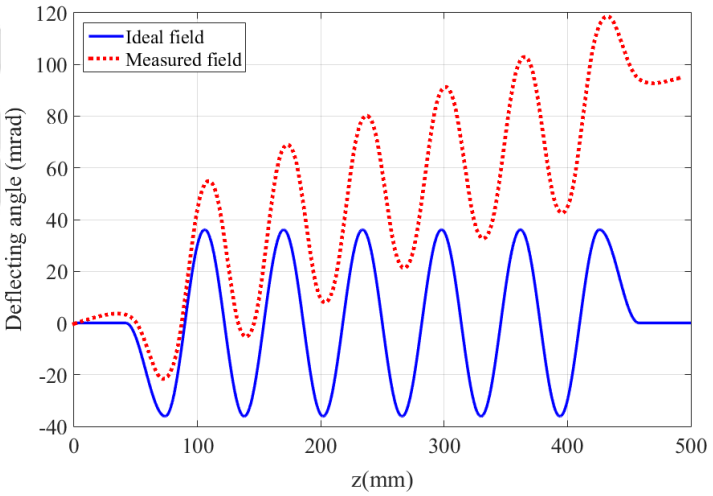

Figure 4.5: Angular displacement or the deflecting angle of 10 MeV electron along the undulator axis for ideal periodic and measured magnetic fields.

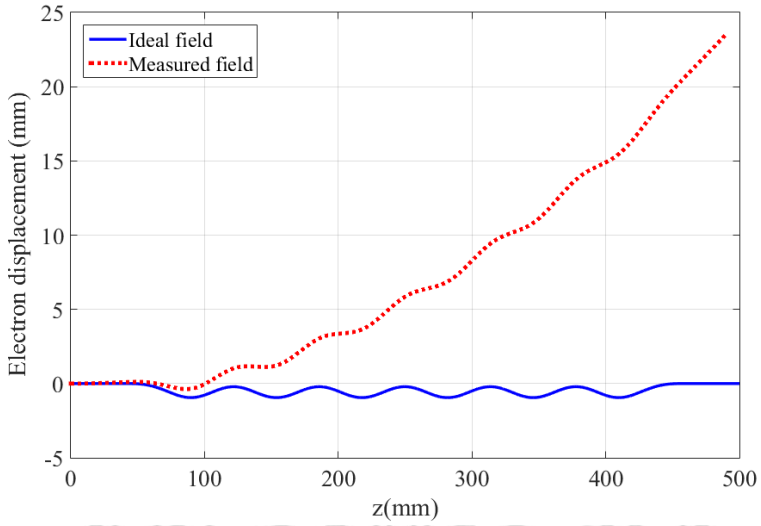

Figure 4.6: Horizontal displacement of 10 MeV electron beam along the undulator axis for ideal periodic and measured magnetic fields.

The deflecting angle and the electron displacement from the measured magnetic field data show that the electron beam departs from the undulator magnet with non-zero deflecting angle and off-axis at the end of the magnet. The deflecting angle and the horizontal displacement of the electron at the undulator exit are around 100 mrad and 24 mm with respect to the mid plane. This is a result of an improper current applied for the end pole conducting coils. The magnetic field integral at two ends of the undulator magnet has to be compensated in order to transport the electron beam in and out the undulator on the central axis. This can be done in the future by adding the resister to the two end coils or by adjusting the end coils' applied current. Furthermore, steering magnets can be used to correct the electrons' movement at the entrance and the exit of the undulator magnet.

The uncompensated end pole field affects significantly to the angular flux density of the undulator radiation. The angular flux densities for both ideal and measured magnetic fields were calculated with the simulation program B2E [43] and the results are shown in Fig. 4.7. When the electron trajectory in the undulator magnet is not parallel to the undulator axis, the emitted radiations from each undulator period destructively add up in the forward direction resulting in the reduction of the radiation intensity. This results that the angular flux density of the measured undulator field is lower than of the ideal periodic magnetic field. Furthermore, the radiation spectrum

does not show the specific peaks corresponding to certain harmonics as suggested in the theory.

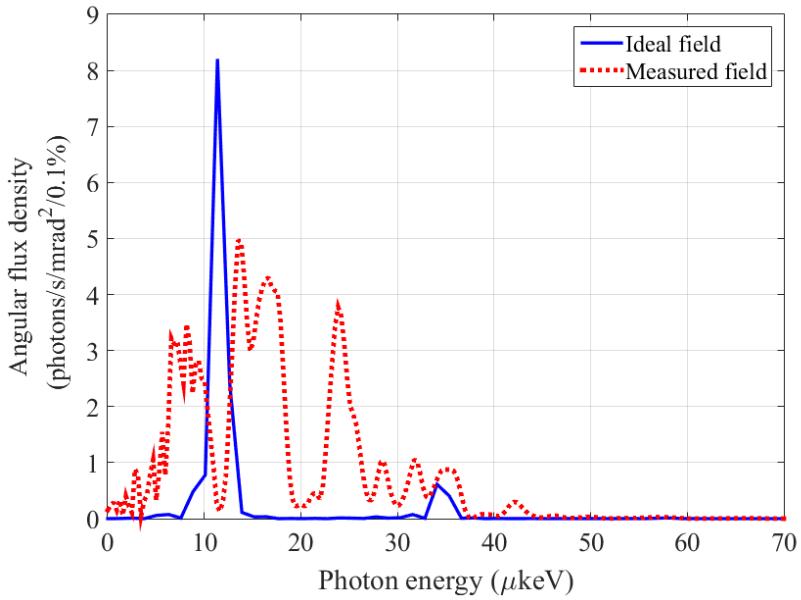

Figure 4.7: Calculated angular flux density as a function of photon energy with electron energy of 10 MeV for ideal periodic and measured magnetic fields.

4.1.3 Undulator Magnet with 30 Periods

I used the results from the prototype undulator to design the undulator magnet with 30 periods for generation of the THz radiation. A 3D RADIA model of the future THz undulator is represented in Fig. 4.8. The ideal magnetic field distribution for the 30 period undulator and electron displacement in this magnet are shown in Fig. 4.9 and Fig. 4.10, respectively. The designed specifications of this 30 period undulator listed in Table 4.1 can be used as the based information for the construction of a future undulator at the PBP-CMU Linac Facility.

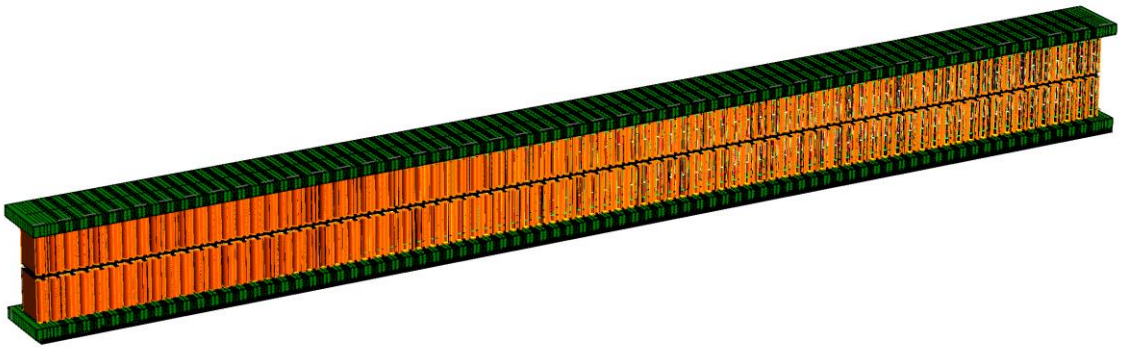

Figure 4.8: 3D RADIA model of the electromagnetic undulator with 30 periods.

Table 4.1: Specifications of the electromagnetic undulator for generation of THz radiation at the PBP-CMU Linac Laboratory.

Parameter	Value
Type	planar
Period length	64 mm
Number of periods	30
Total length	1.92 m
Magnetic gap	10.5 mm
Peak magnetic field	50 - 167 mT
Undulator parameter (K)	0.3 - 1.0

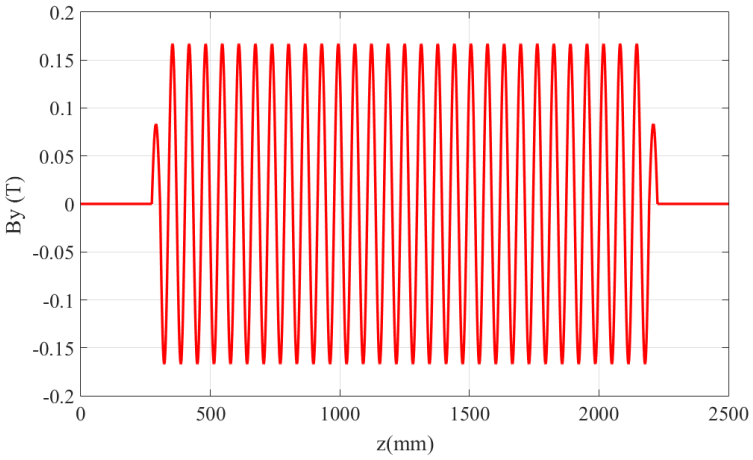

Figure 4.9: Ideal magnetic field distribution along the longitudinal distance of the undulator magnet with 30 periods.

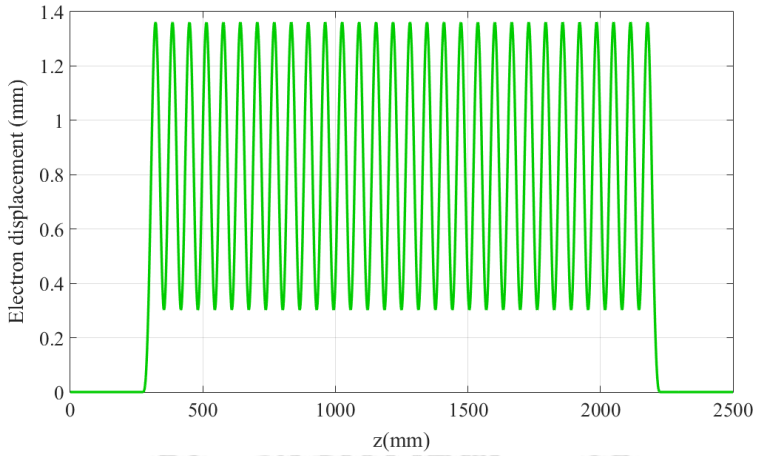

Figure 4.10: Electron displacement of 10 MeV electron beam traveling through an ideal periodic magnetic field of the 30 period undulator.

The radiation spectrum for 30 period undulator magnet simulated with program B2E for the ideal sinusoidal magnetic field is shown in Fig. 4.11. The ideal angular flux density is calculated from the 10 MeV electron beam and the peak undulator field of 167 mT. The result shows that the angular flux density at the fundamental harmonic is dominated at the photon energy of around 10 meV with a quasi monochromatic peak.

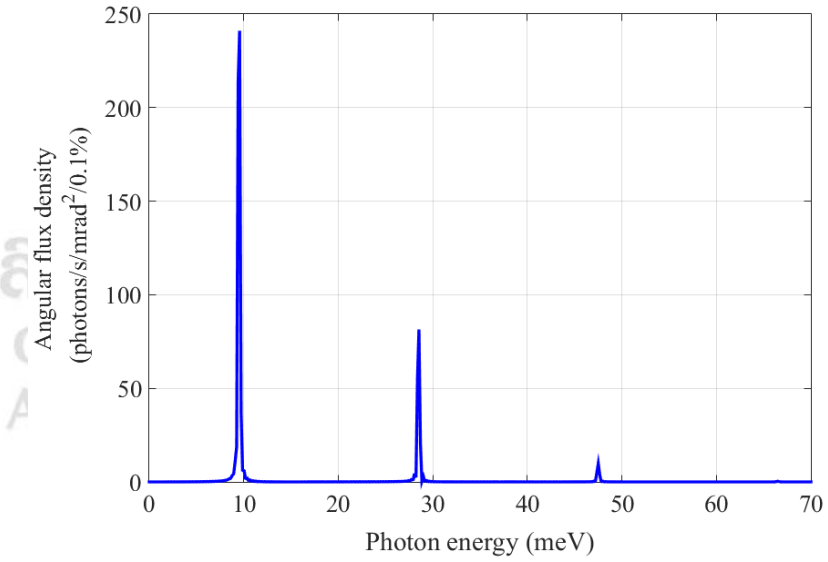

Figure 4.11: Angular flux density as a function of photon energy with electron energy of 10 MeV for ideal periodic magnetic field of 30 period undulator.

4.2 Undulator Radiation

4.2.1 Radiation Wavelength

The dependence of the radiation wavelength on the undulator parameter and the electron beam energy was considered for 5, 7, 10, 15, and 20 MeV electron beams. The first harmonic radiation wavelength and the undulator parameter were determined by using Equation (2.59) for on-axis radiation. The undulator magnet with specifications listed in Table 4.1 was employed in this calculation. The radiation wavelength as a function of the undulator parameter for different electron beam energies is shown in Fig. 4.12.

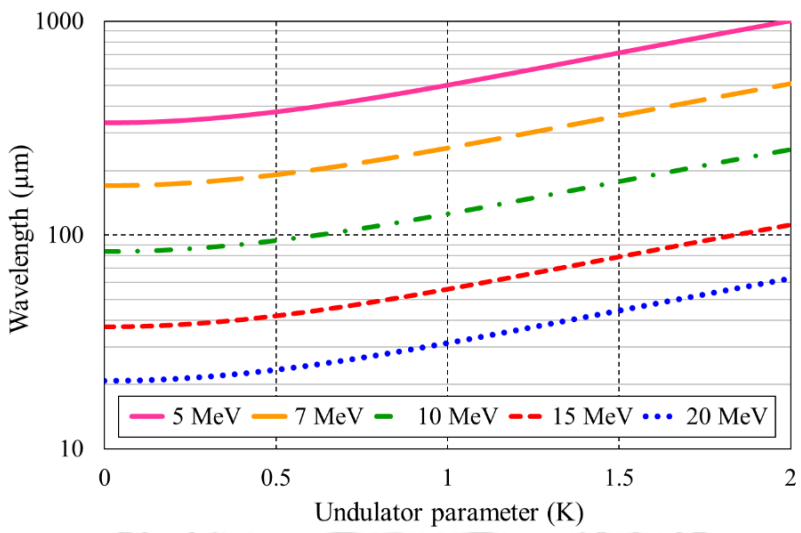

Figure 4.12: Undulator radiation wavelength as a function of undulator parameter for electron energies of 5, 7, 10, 15 and 20 MeV.

The undulator parameter can be varied by adjusting the magnetic field of the undulator magnet with a specific undulator period length. The radiation wavelength is longer when the undulator parameter increases for the same electron energy. Figure 4.12 reveals that low-energy electron beam is suitable for production of the undulator radiation with long wavelength. On the other hand, high-energy electron generates short wavelength radiation. The radiation wavelength of around 80 - 115 μm can be obtained when using the undulator magnet with an undulator parameter of 0.3 - 1 for the 10 MeV electron beam.

The electron bunch length as a function of the bunch form factor for the radiation wavelength of 100, 500, and 1000 μm is presented in Fig. 4.13. The

calculation results show that the form factor decreases and approaches to 1 when the electron bunch length reduces. The maximum limit of the electron bunch length to generate the coherent radiation is different for each radiation wavelength. For shorter radiation wavelength, the form factor approches zero at short bunch length. Consequently, the electron bunch length should be equal or shorter than the radiation wavelength with the factor of 2π in Equation (2.82) for producing the coherent radiation.

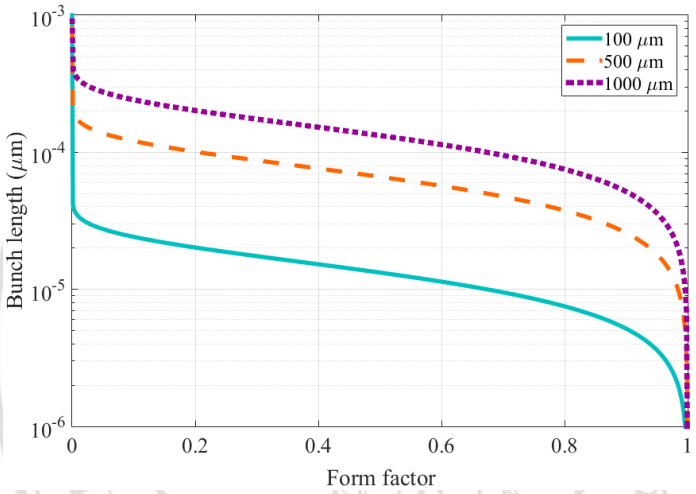

Figure 4.13: Electron bunch length versus the bunch form factor for radiation wavelength of 100, 500, and 1000 μm.

4.2.2 Radiation Average Power vs. Electron Beam Energy

Firstly, the measured properties of electron beam after the linac acceleration (Table 3.4) and specifications of the undulator magnet in Table 4.1 were used to calculate the power of the undulator radiation. The beam size and divergence of the electron beam were not measured in the experiment and their values were then assumed to be small. A relative spectral bandwidth $(\Delta\omega/\omega)$ for the fundamental harmonic was determined from the number of undulator periods, which is $\Delta\omega/\omega = 1/N_u$. Thus, the spectral bandwidth of 3%BW was used to calculate the radiation power in this study. It is noted that all powers presented in this chapter are an average power following Equation (2.84) for the undualtor radiation and Equation (2.95) for the transition radiation.

Practically, the electron trajectory in the undulator magnetic field is not exactly sinusoidal and hence the emitted radiation includes both fundamental and higher harmonics. The specific central wavelength can be calculated for each harmonic following Equation (2.59). The spectral average power of the radiation produced from the electron beam with measured beam parameters for the undulator parameter of 1 at the first three harmonics are shown in Fig. 4.14. The radiation spectrum shows that the radiated power of the first harmonic is maximum, which is the principle characteristic of the undulator radiation for the undulator parameter around 1 $(K \approx 1)$. The radiation with higher harmonic has shorter central wavelength with lower radiated power.

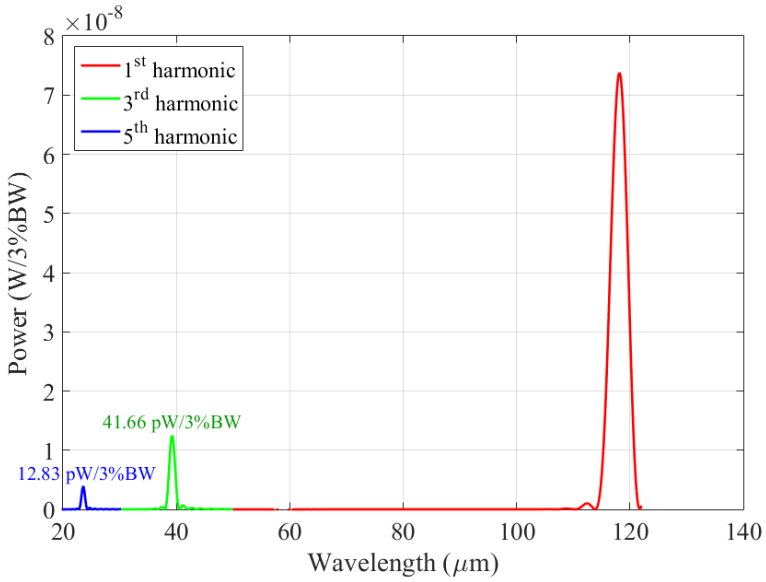

Figure 4.14: Radiated average power of the first three harmonics of undulator radiation as a function of radiation wavelength for the electron beam with measured properties shown in Table 3.4.

As shown in Table 4.1, the undulator parameter considered in this study is in the range of 0.3 - 1. The radiated power and central wavelength at the first harmonic of radiation spectrum for the undulator parameter from $K = 0.3$ to $K = 1$ was calculated and plotted in Fig. 4.15. The radiated power from the undulator magnet with $K = 1$ is about 10^3 times higher than that of the undulator magnet with $K = 0.3$.

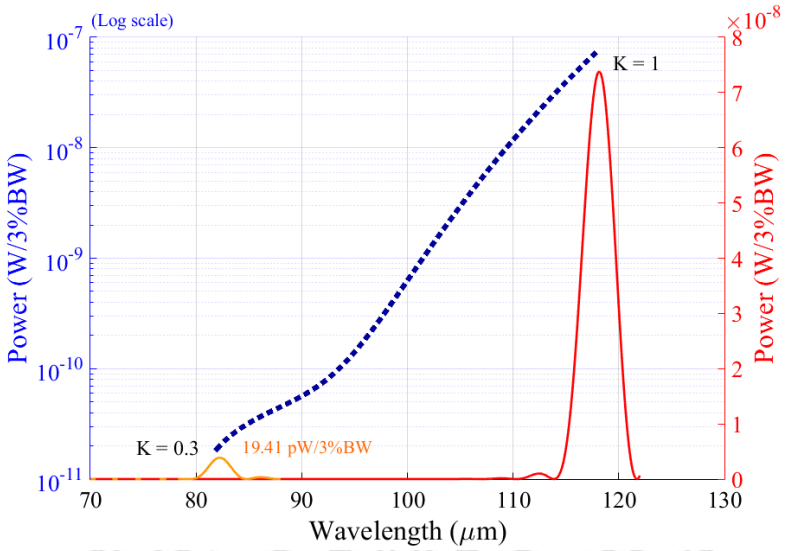

Figure 4.15: Spectral average power at fundamental harmonic of the undulator radiation from 9.81 MeV electron beam with the undulator parameter from $K = 0.3$ to $K = 1$.

Furthermore, the powers of undulator radiation at the fundamental harmonic for electron beam energies of 8, 10, 12 MeV without the limitation of the undulator parameter are shown in Fig. 4.16 (left). The spectral powers for all electron beam energies are continuous and cover broad wavelength range. The radiated power gradually decreases when the wavelength reduces. The spectral power at long wavelength for all electron beam energies are rather the same. Electron beams with higher energies generate the undulator radiation with broader wavelength range. When the value of the undulator parameter is only limited in the range of $K = 0.3$ to $K = 1$, the undulator radiation of higher beam energy covers shorter wavelengths with lower spectral power as shown in Fig. 4.16 (right). The electron beams with kinetic energies of 8 MeV and 12 MeV can respectively generate the undulator radiation in THz or MIR regime, while the electron beam with energy of 10 MeV can produce both THz and MIR radiation.

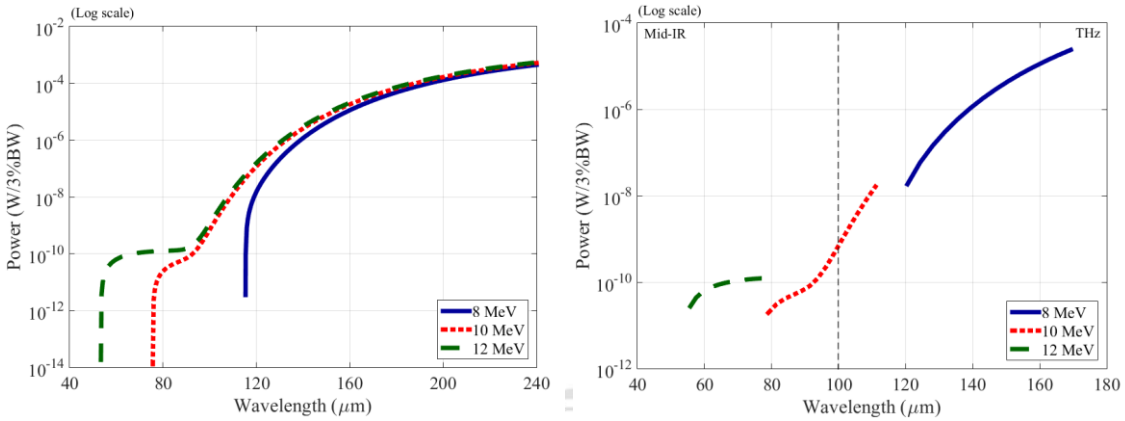

Figure 4.16: Spectral average power of undulator radiation at fundamental harmonic for electron beam energies of 8, 10 and 12 MeV without limitation of undulator parameter (left) and with the undulator parameter range of $K = 0.3$ to $K = 1$ (right).

4.2.3 Radiation Average Power vs. Electron Bunch Length

Dependency of electron bunch length on the undulator radiation power was studied for the electron beam with energy of 9.81 MeV. The 3%BW radiated power at the fundamental harmonic for different electron bunch lengths are illustrated in Fig. 4.17. Based on the measured beam properties in Table 3.4 and the undulator magnet specifications in Table 4.1, the minimum radiated wavelength for all electron bunch lengths is 80 μm due to the limitation as expressed in the term $2n\gamma^2\lambda_r - \lambda_u$ in Equation (2.84). Thus, the undulator radiation from the electron beam with a bunch length of 45 and 65 μm has only the contribution from the coherent radiation. While the radiation from the beams with bunch lengths of 85, 105, and 200 μm consists of both incoherent and coherent radiations. The coherent radiation is 10^8 times (N_e times) higher than the incoherent part. This agrees well to the theoretical suggestion that the coherent radiation is proportional to the number of electrons squared, while the incoherent radiation is proportional to the number of electrons. As shown in Fig. 4.17, the average powers of all cases increase logarithmically and then saturate up to about 2 mW/3%BW at the long radiation wavelength of 800 μm. The power for long wavelength saturates because the form factor approaches infinity. An electron beam with shorter bunch length generates undulator radiation with a broader spectrum and higher radiation power for wavelengths shorter than about 700 μm.

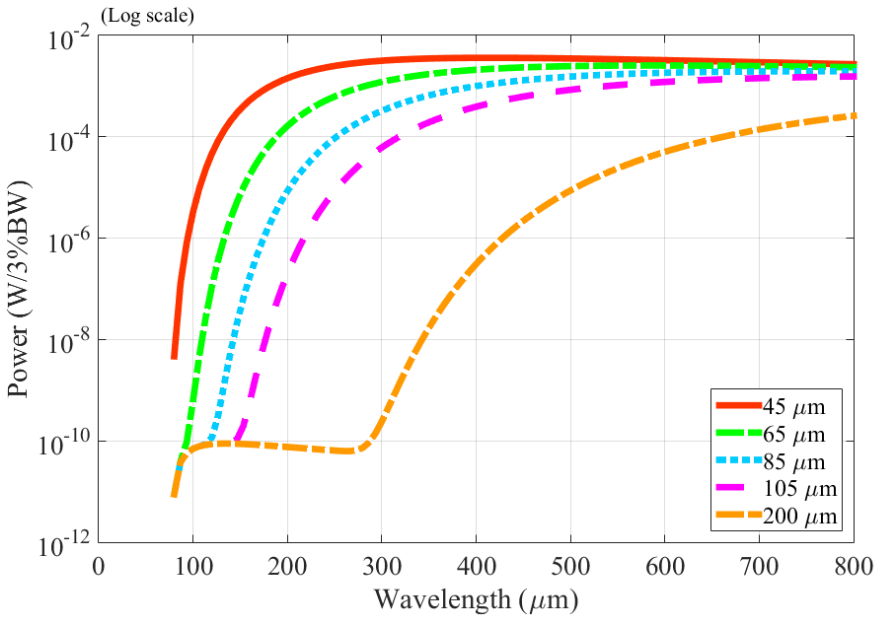

Figure 4.17: Spectral power of undulator radiation at fundamental harmonic for electron beam with the bunch lengths of 45, 65, 85, 105, and 200 μm.

In practice, when we consider the undulator parameter in the available range of $K = 0.3$ to $K = 1$, the possible radiated wavelengths are limited in shorter range as shown in Fig. 4.18. The electron beams with the bunch lengths of 85, 105, and 200 μm generate incoherent undulator radiation with lower radiation power compared to electron beams with bunch length shorter than the radiation wavelength. The electron beam with the bunch length of 45 μm generates purely coherent radiation since its bunch length is much shorter than the radiation wavelengths. While the electron beams with the bunch lengths of about or longer than 65 μm can produce both coherent and incoherent radiation as clearly seen in Fig. 4.17. Figures 4.13 and 4.18 reveal that the PBP-CMU Linac system should be able to produce the electron beam with the bunch length equal or shorter than 45 μm (150 fs) in order to achieve the coherent undulator radiation at the central wavelength of longer than 100 μm.

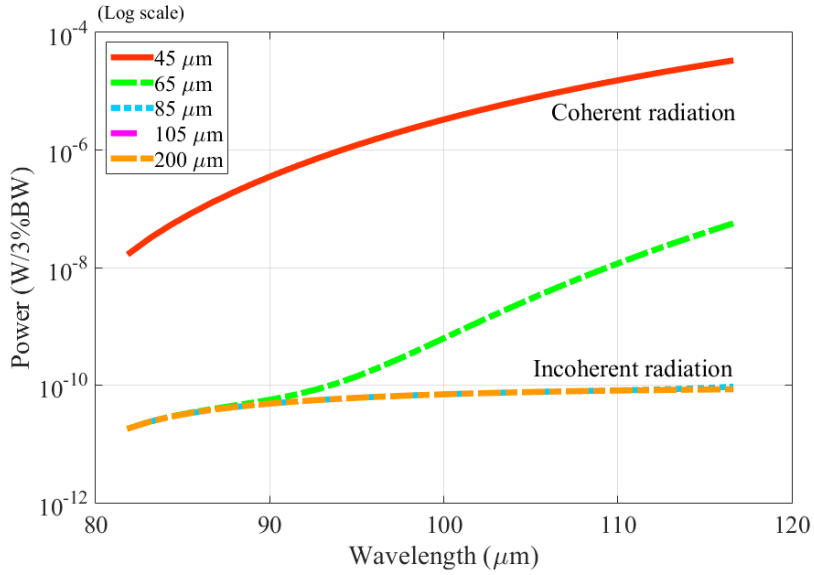

Figure 4.18: Radiated spectral power at fundamental harmonic for the electron beams with different bunch lengths for undulator parameters of $K = 0.3$ to $K = 1$.

4.2.4 Radiation Average Power vs. Electron Bunch Charge

An electron bunch charge is one of the most important parameters for generation of coherent undulator radiation. The spectral power of the radiation for the first three harmonics generated from the electron beams with different bunch charges are shown in Fig. 4.19. The radiated wavelength is varied as a function of the undulator parameter in the range of $K = 0.3$ to $K = 1$. We used the electron beam with an energy of 9.81 MeV and a bunch length of 65 μm (217 fs) for all calculations in this section.

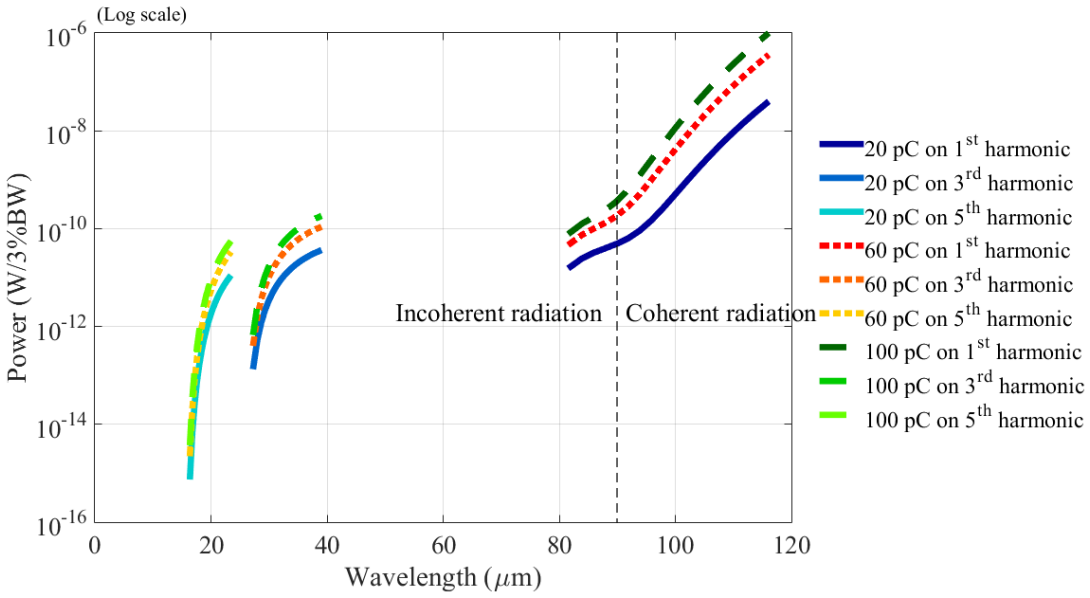

Figure 4.19: Radiated power for the first three harmonics of undulator radiation produced from electron bunch charges of 20, 60, 100 pC with the undulator parameter in the range of $K = 0.3$ to $K = 1$. The radiation with wavelengths longer than 90 μm is the coherent radiation, while the radiation with wavelengths shorter than 90 μm has only the incoherent contribution.

The radiated power is obviously higher as the bunch charge of the electron beam is larger. The emitted radiation at the fundamental harmonic displayed in Fig. 4.20 shows that the spectral power rapidly increases for the electron bunches with low charges and increases with constant rate at high bunch charge. The radiations with wavelengths longer than 90 μm show the feature of coherent radiation, which the power is proposional to $N_e(N_e - 1) f(\omega)$. Contradictory, the radiation with wavelengths shorter than 90 μm has only the incoherent contribution, which is a result of the factor N_e in Equation (2.84).

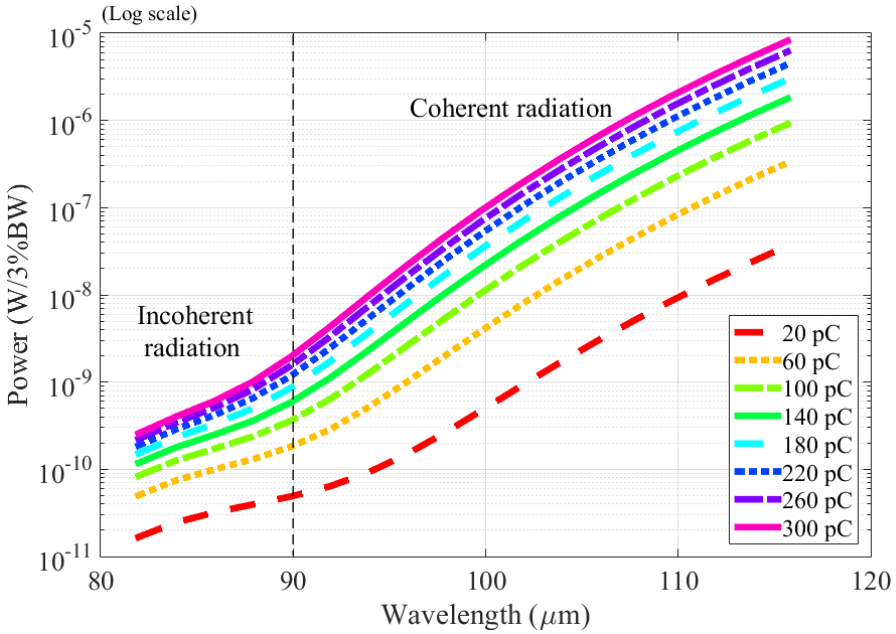

Figure 4.20: Spectral power for the undulator radiation at the fundamental harmonic for different electron bunch charges with undulator parameters in the range of $K = 0.3$ to $K = 1$. The radiation with wavelengths longer than 90 μm is the coherent radiation, while the radiation with wavelengths shorter than 90 μm has only the incoherent contribution.

4.2.5 Comparison between Measurement and Simulation Results

Electron beam properties in Tables 3.4 and 3.5, which are the measurement result, the simulated result for the measurement conditions and the simulated result for the optimal operating perameters, were used to calculate the spectral power of the undulator radiation. The major difference between the measurement and the simulation is that in the measurement the electron beam has a bunch charge (22.4 pC) much smaller than the simulation (110.4 pC). The radiated powers for these three cases without the limitation of the undulator parameter are shown in Fig. 4.21. It shows that the spectral powers of both simulated results are higher than that of the measurement one at long radiation wavelengths due to higher bunch charge. At the radiation wavelength shorter than 350 μm, the measurement case with electron bunch length of 65 μm has higher radiation power than the simulation with measurement conditions, which has the electron bunch length of 116 μm. This is due to the effect of shorter electron bunch length. Moreover, it is clearly seen that for the simulation with measurement conditions the radiations with wavelengths shorter than about 160 μm have only incoherent contribution.

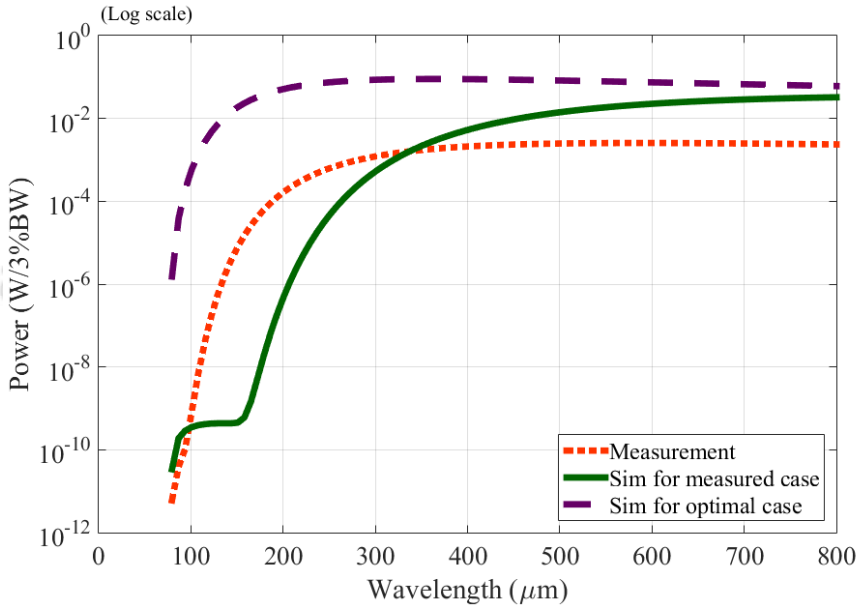

Figure 4.21: Radiated power of the undulator radiation at fundamental harmonic for electron beam properties in cases of measurement, simulation with measurement conditions, and simulation with optimal operating parameters.

When we consider the power of radiation from the undulator magnet with the undulator parameter in the range of $K = 0.3$ to $K = 1$, the radiation powers for all cases at higher harmonics have large contribution of the incoherent radiation for the radiation wavelength shorter than 40 μm as shown in Fig. 4.22. This is because the beams have long bunch lengths compared to the radiation wavelengths in the consider range. For the radiation wavelength longer than 80 μm, the electron beam in the case of simulation with optimal parameters radiates coherently.

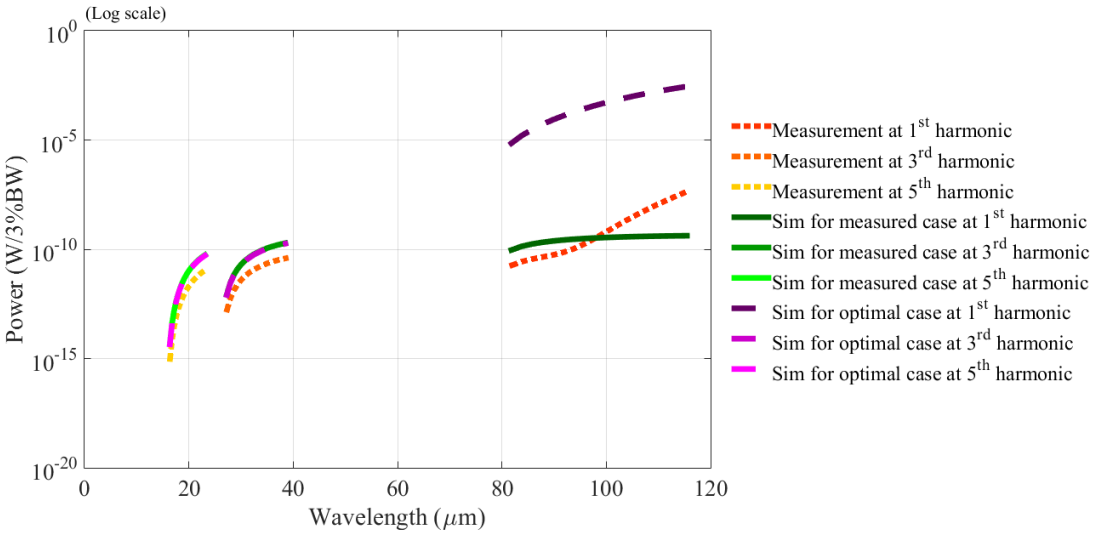

Figure 4.22: Radiated power of the undulator radiation at the first three harmonics with undulator parameters in the range of $K = 0.3$ to $K = 1$ for three considered cases.

It is clearly seen in Figs. 4.21 - 4.22 that the electron beam in the case of simulation with optimal operating parameters can generate the undulator radiation at the fundamental harmonic with highest spectral power. The calculated average power of this case from the undulator magnet with $K = 1$ reaches 2.81 mW for 3%BW. This is about 10^4-10^5 times higher than the case of the beam with measured beam properties for radiation wavelengths shorter than 120 μm. The difference is reduced to 10-1000 times when the radiation wavelength is longer than 120 μm. Furthermore, the radiation powers at higher harmonics for both simulation cases are higher than that of the measurement one at the same wavelengths.

4.2.6 Comparison between Undulator Radiation and Transition Radiation

The spectral average power of the undulator radiation and the transition radiation produced from electron beams with 3 considered cases, which are measurement, simulation with measurement conditions and simulation with optimal operating parameters, were calculated. The study results of all cases are shown in Figs 2.23 - 2.25. The average power of the undulator radiation was considered for the radiation in a central cone from the electron beam with longitudinal Gaussian distribution. The average power of the transition radiation was calculated by using Equation (2.95) for the electron beam moving across the boundary between vacuum and Al-foil.

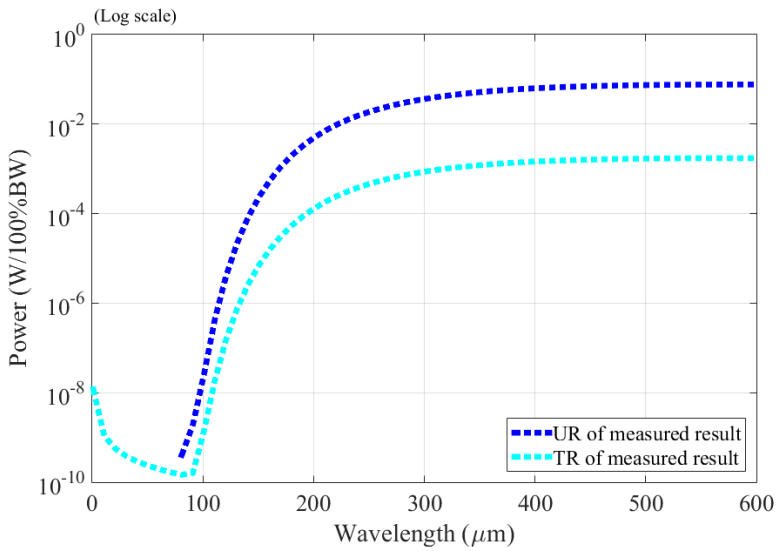

Figure 4.23: Comparison of radiation average powers of the undulator radiation (UR) and the transition radiation (TR) for electron beams with the properties obtained from the measurement (Table 3.4).

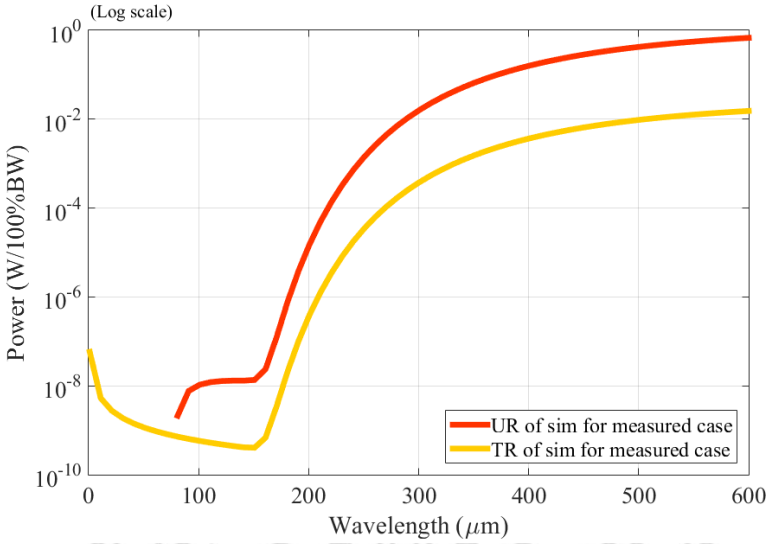

Figure 4.24: Average powers of undulator radiation (UR) and transition radiation (TR) for electron beams with the properties obtained from the simulation for the measurement conditions.

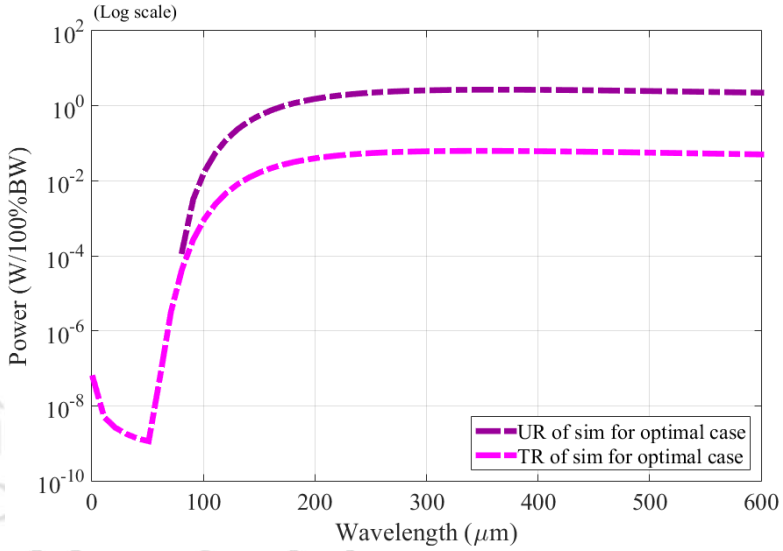

Figure 4.25: Average powers of undulator radiation (UR) and transition radiation (TR) for electron beams with the properties obtained from the simulation for the optimal operating perameters.

The results in all three figures show that the average power of the coherent undulator radiation is about 50 times higher than the coherent transition radiation for the radiation wavelength longer than 200 µm. However, the transition radiation can be produced with longer wavelength range covering from THz to MIR regimes, while the

undulator radiation produced from the undulator magnet with undulator parameters in the range of $K = 0.3$ to $K = 1$ covers only the THz regime.